3246–3252 *Nucleic Acids Research, 1996, Vol. 24, No. 16*

Kinetics of spontaneous displacement of RNA from heteroduplexes by DNA

Ralf Landgraf*, Kumaran S. Ramamurthi and David S. Sigman

Department of Chemistry and Biochemistry, Molecular Biology Institute, University of California, Los Angeles, CA 90024-1570, USA

Received April 1, 1996; Revised and Accepted June 25, 1996

ABSTRACT

We have used R-loop formation and direct hybridization techniques to analyze the kinetics by which RNA is displaced from a heteroduplex by DNA of identical sequence. Using random walk simulations we were able to calculate the step times for a single displacement reaction. For RNA with a GC content of 57–60% the data indicate an RNA exchange probability of 50.06%, which is indicative of a modest destabilization of the heteroduplex compared with a DNA duplex in the presence of magnesium. The average step time for the reversible exchange of a single nucleotide is 345.0 (± 1.3) ms/step. An acceleration of the displacement reaction was observed in the absence of magnesium. A comparison with step times for elongation shows that RNA displacement would not be rate limiting to transcription elongation under two conditions: (i) if magnesium is eliminated from the newly synthesized heteroduplex; (ii) if displacement is kept in a forward only exchange mode through binding of the emerging RNA. Distamycin, a minor groove binding drug, is very effective as a 'catalyst' of RNA displacement. This effect is likely to be due to preferential binding of distamycin to the minor groove of the DNA duplex as opposed to the heteroduplex. This kinetic assay could therefore serve as a convenient assay for the determination of binding preferences of nucleic acid ligands.

INTRODUCTION

Heteroduplexes consisting of 1 mol RNA and 1 mol DNA form *in vivo* during reverse transcription, transcription and replication. Although they played a historically important role in the discovery of the exon/intron structure of transcription units and are central in the design of antisense deoxyoligonucleotides, their kinetic and thermodynamic stability has not been extensively investigated. Structurally, heteroduplexes prefer an intermediate topology close to an A-form helix (1,2). Determination of the thermodynamic properties of heteroduplexes relative to their homoduplex counterparts is complicated by the greater sequence-dependent variation in thermal stability encountered for different RNA–DNA pairs (3). Overall, mixed sequence heteroduplexes are reported to have reduced thermodynamic stability compared with double-stranded B-form DNA or A-form RNA (3–5).

R-loop formation, i.e. sequence-specific local displacement of one strand of DNA from a duplex structure by RNA of identical sequence, provides a defined starting material for kinetic analysis of the exchange reaction between these two helices. The sequence-specific formation of R-loops at elevated temperatures (50–60°C) in 70% formamide is driven by the higher thermodynamic stability of RNA–DNA duplexes compared with double-stranded DNA under these solvent conditions (6,7). The exact nature of this increased stability is not fully understood. However, a possible driving force for this exchange could be the higher extent of hydration of the minor groove of B-form DNA compared with the A-form (8). Organic solvents therefore tend to force DNA into the less stable A-form. This decreased stability is reflected in a tendency to unwind upon dehydration (9). Thus solvent-enforced A-form DNA would become less stable than a heteroduplex, which can remain in its preferred topology, resembling the A-form. The high stringency of this hybridization reaction makes R-loop formation a useful tool for the identification of transcribed genomic sequences (10,11) and sequence-specific scission of DNA (12,13).

After removal or dilution of formamide, the thermodynamic advantage of heteroduplex formation is lost and DNA gradually displaces RNA from the R-loop structure in a strongly temperature-dependent manner (6,14). While this instability presents a problem for reactions requiring intact R-loops, it also provides an opportunity to study the kinetics of strand exchange. The conditions under which heteroduplex formation is thermodynamically favored and the conditions for RNA displacement are mutually exclusive, yet easily convertible. This provides a clear starting point for kinetic analysis. We previously presented a study on the impact of RNA length and the use of charge-modified nucleotides on R-loop formation and stability (14). The analysis of R-loop stability as presented in this earlier publication included a model for the displacement of RNA that was based on a random walk model. This model has been applied successfully to the exchange of DNA by DNA in triple-stranded test systems (15) and protein-free Holliday junctions (16,17). In this present communication we analyze the kinetics for the displacement of RNA from R-loop structures by competing DNA and compare the estimated step times with rates for fast transcription elongation. In addition, we demonstrate the effect of

* To whom correspondence should be addressed

the minor groove binding reagent distamycin on the exchange rate. We demonstrate that this assay can be used to analyze the helix topology-based binding preferences of reagents that bind to double-stranded nucleic acids.

MATERIALS AND METHODS

RNA synthesis

RNA was generated *in vitro* as described earlier using run-off transcription on linearized pGEM-820 or pGEM-4 plasmids (13,18).

R-Loop formation

R-Loops were formed as described previously (13,18) with the exception that substrate plasmid was linearized in such a way that half open R-loops were obtained (Fig. 1). A 50 µl R-loop reaction contained 1 pmol linearized plasmid, 1–10 pmol RNA, 70% deionized formamide, 83 mM PIPES, pH 7.8, 33 mM NaCl and 10 mM EDTA. The reaction was heated to 55°C in a thermocycler and the temperature was lowered to 45°C over a period of 4 h. [Formamide was redistilled nucleic acid grade from BRL. Aliquots were deionized over BioRad mixed bed resin AG 501-X8(D) and stored at –20°C.] For oligonucleotide-based R-loop reactions RNA was generated from the T7 promoter on *Eco*RI linearized pGEM-4 (Pharmacia). This RNA was subsequently annealed to gel-purified pGEM-4-based synthetic oligonucleotides. The 89 nt 'template strand' (5′-TGACACTAT AGAATACACG GAATTCGAGC TCGGTACCCG GGGATC-CTCT AGAGTCGACC TGCAGGCATG CAAGCTTCCG GTCTCCCTA-3′) anneals to the entire 66 nt RNA transcript (underlined sequence) and provides a 20 nt 5′ overhang which allows annealing of the 90 nt 'non-template strand' (3′-ATC-CACTGTG ATATCTTATG TGCCTTAAGC TCGAGCCATG GGCCCCTAGG AGATCTCAGC TGGACGTCCG TACGTT-CGAA GGCCAGAGGG-5′) (double underlined sequence is in competition with RNA for binding to the template strand).

Strand exchange assays by gel shift analysis

RNA was radiolabeled by the addition of [α-^{32}P]GTP during transcription. *Nhe*I- or *Sph*I-digested pGEM-820 was used as the substrate for the transcription reaction as well as the template for formation of R-loops of 311 and 545 bp respectively. R-Loop formation and the initiation of strand exchange were carried out as described above. After a 10-fold dilution of the R-loop reaction with 1.1× RB (20 mM Tris–HCl, pH 7.4, 5 mM $MgCl_2$, 50 mM KCl), 30 µl aliquots were removed at different time points, mixed with 30 µl ice-cold stop solution (RB plus 1 mg/ml ethidium bromide) and placed on ice. (The addition of ethidium bromide to the stop solution and electrophoresis buffer was based on published protocols for DNA strand migration analysis. For heteroduplex analysis ethidium bromide was later found to destabilize the R-loop at 37°C. However, sufficient stabilization of the complex is achieved through the presence of magnesium and the low temperature that was maintained after stopping the reaction.) Samples were electrophoresed at 4°C on a 0.8% agarose gel in TBE buffer containing 0.5 µg/ml ethidium bromide and 5 mM magnesium chloride.

Strand exchange assay by restriction digest interference

For oligonucleotide based assays, radiolabeled 'template strand' oligonucleotide (14.4 pmol) was annealed to RNA (130 pmol) and non-template strand oligonucleotide (147 pmol) under standard R-loop formation conditions. After R-loop formation was completed, we induced strand exchange by diluting this 60 µl reaction 10-fold with 1.1× RB, prewarmed to 37°C. To keep data obtained by different methods comparable, this restriction digest buffer was used for all subsequent experiments. Aliquots (30 µl) of this reaction were removed at different time points and were digested through the addition of 20 U *Hinc*II for 1 min. The partial restriction digest was stopped by the addition of EDTA (final concentration 10 mM). Aliquots were analyzed through denaturing polyacrylamide gel electrophoresis, autoradiography and densitometry. The restriction digestion with *Eco*RI was carried out in the same way using R-loop-containing plasmid DNA as the substrate. RNA was incubated in an ~3-fold excess over the *Nhe*I-digested end-labeled plasmid. Analysis of the products was carried out through agarose gel electrophoresis.

Random walk simulation

An array was defined to contain the information for 100 R-loops. Any element in this array has a position marker assigned representing the position of the junction relative to the length of the RNA. To simulate one step in a random walk the value of each position marker was independently modified one integer up or down based on whether a randomly drawn number between 1 and 100 fell below or above a preset threshold representing the RNA exchange probability. For R-loops at the starting position (no RNA exchanged) only displacement of RNA is scored. Elements for which the position of the marker equals the length of the RNA were removed from the simulation and scored as completely exchanged. The course of a single exchange reaction as presented in Figure 3A was simulated on a PC using a program written in Quick Basic (Microsoft). All other calculations involve averaging of 10–20 simulations using a program written in C (Borland).

RESULTS

Analysis of the displacement reaction by gel mobility shift assays

The general outline of the assay system used for measurement of RNA displacement by DNA is shown in Figure 1. *Nhe*I-linearized plasmid serves both as the template for RNA synthesis as well as the substrate for R-loop formation. Restriction sites present in pGEM-820 and pGEM-4 provide a convenient method for the preparation of RNAs of different length. The use of the same linearized plasmid during R-loop formation yields a truncated, open loop and ensures that displacement of the RNA through DNA strand migration is initiated on one flank only. Although displacement through unchallenged dissociation of RNA and replacement by excess free DNA provides a mechanism of strand exchange at the open side of the loop, this reaction is very slow and inefficient compared with exchange by branch migration. This is evident from the stable coexistence in solution of heteroduplexes and competing DNA in the absence of an accessible and complementary sequence between both DNA strands that allows initiation of a branch point (data not shown). The strong temperature dependency of the exchange reaction (16,19) enables visualization of the displacement by a gel mobility shift assay that was modified based on the

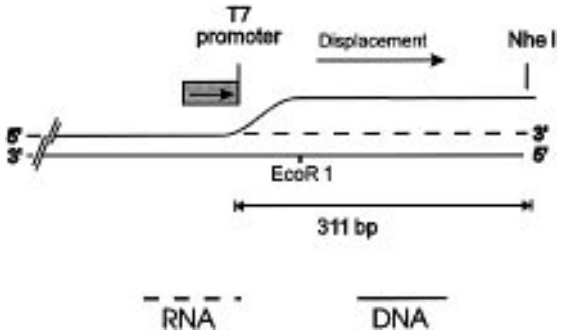

Figure 1. Schematic of a truncated R-loop used for the displacement assay. *Nhe*I-digested pGEM-820 is used to generate the 311 nt RNA transcript from the T7 promoter. The same linearized plasmid and purified RNA are used as substrates for R-loop formation. The resulting 'R-loop' is truncated and displacement will occur 'unidirectionally'. Restoration of the *Eco*RI site, located at position 66 of the RNA transcript, is used in the restriction digest interference assay to confirm the directionality of exchange.

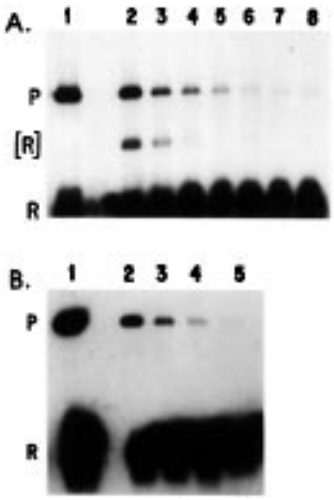

Figure 2. (**A**) Gel mobility shift assay of the displacement of a 311 nt RNA (*Nhe*I-digested pGEM-820 template of Fig. 1) in the presence of 5 mM magnesium. Samples 2–8 were removed at various time points after dilution of the R-loop reaction, stopped on ice and analyzed by agarose gel electrophoresis at 4°C. Sample 1 (lane 1) was loaded directly from the R-loop mix without dilution of formamide or storage on ice. Lanes 1–8, incubation times at 37°C were 0 , 0.5 , 2, 4, 6, 8, 12.75 and 24 h. The positions of the plasmid and RNA are labeled P and R respectively. [R], a product of RNA self-association. (**B**) Gel mobility shift assay of the displacement of the same 311 nt RNA in the absence of magnesium. Lanes 1–5, incubation times at 37°C were 0, 2, 5, 10 and 20 min. The positions of the plasmid and RNA are labeled P and R respectively.

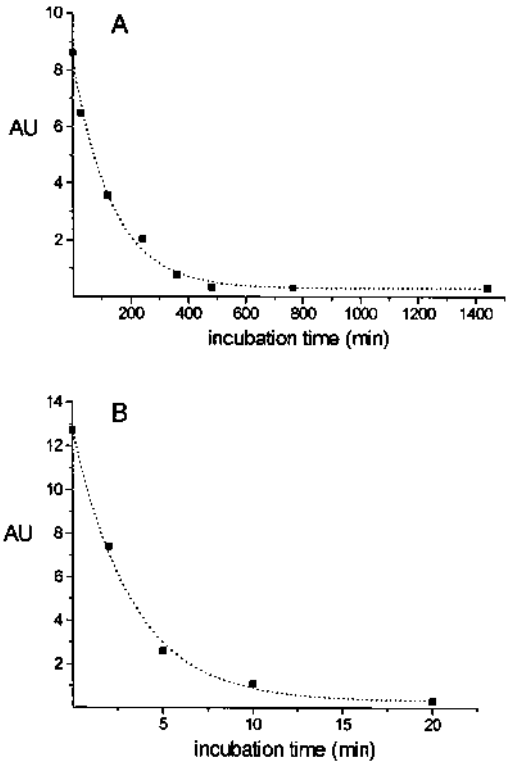

Figure 3. (**A**) Signal decay of pGEM-820-associated radioactivity from Figure 2A (exchange in the presence of 5 mM magnesium), determined by densitometry. (**B**) Signal decay of the plasmid-associated radioactivity from Figure 2B (exchange in the absence of magnesium).

corresponding assay used by Panyutin *et al.* for the analysis of DNA displacement. In this assay, the association of radiolabled RNA with the plasmid band is followed through agarose gel electrophoresis.

Figure 2A shows the displacement of a radiolabeled 311 nt RNA, visualized by a gel mobility shift. After R-loop formation with *Nhe*I-linearized plasmid, a 10-fold dilution of the R-loop formation mixture with prewarmed aqueous buffer (RB) containing a final magnesium concentration of 5 mM initiates strand displacement. The control (lane 1) shows an R-loop reaction which was directly applied to the precooled agarose gel without dilution of formamide and storage on ice. The single band identified in this control matches the location of the linearized plasmid as identified by ethidium bromide staining. The additional band visible at short time points (lanes 2 and 3) represents a non-plasmid-related and unstable product of RNA self-association found only after formamide dilution in a Mg^{2+}-containing buffer and prolonged storage on ice prior to electrophoresis. A graphical representation of the displacement of RNA from the plasmid band (Fig. 3A) shows a signal decay with a half-life of ~130 min. A comparison with R-loops that were ethanol precipitated and resuspended in the cold to remove formamide entirely showed that the displacement that occurred after increasing the reaction temperature to 37°C proceeded in the same manner as was observed after 10-fold dilution of formamide. This is consistent with the assumption that the remaining 7% formamide after dilution of the R-loop reaction is below the threshold necessary to keep the DNA helix in the destabilized A-form. In order to reduce the risk of R-loop instability caused by warming up of the sample during the precipitation and washing steps, strand exchange was initiated by formamide dilution in subsequent experiments. The exchange reaction exhibits a strong sensitivity towards magnesium ions. If the reaction is carried out in the absence of magnesium chloride, the displacement reaction is accelerated 52-fold (t½ 2.5 min) (compare Figs 2A and 3A with 2B and 3B).

Random walk simulation, outlined previously (14,16), bridges the gap from the empirical half-lives of R-loops formed with RNAs of different length to the 'step time', the time necessary for the reversible exchange of a single nucleotide. Displacement of the RNA by DNA is simulated by assuming that the branch point of the displacement reaction can move upstream, thereby displacing the DNA by RNA, or vice versa. In this system, the number of steps required for exchange of the hybridized RNA

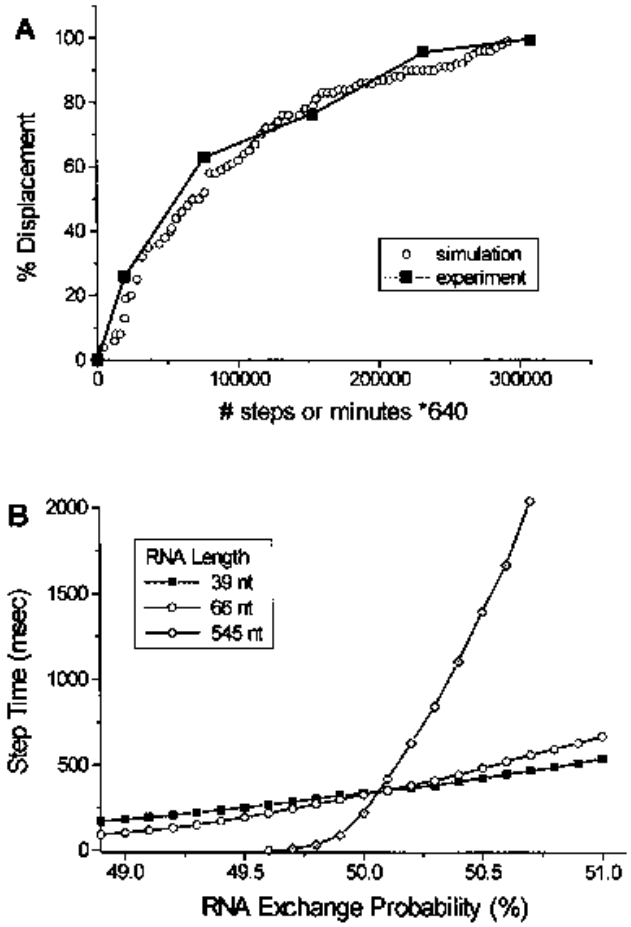

Figure 4. (**A**) Comparison of experimental results for the displacement of the 311 nt RNA with a random walk simulation. Both presentations are synchronized to the time point or step number when displacement was first observed. Gel mobility shift data from Figure 3A have been converted from optical density data of the retarded band into percentage displacement. (**B**) Plot of step times, calculated based on the experimental half-life and the number of steps for half complete displacement in a random walk simulation versus RNA exchange probability. Average values from 20 simulations are presented for RNA of three different lengths but comparable sequence composition (see Table 1).

depends on the length of the RNA and the exchange probability for branch migration in either direction.

In a random walk simulation of the displacement of a 311 nt RNA at 50% RNA exchange probability (i.e. equal probability for the displacement of RNA by DNA and the reverse reaction) half of the RNA population is completely displaced after 82 000 steps. The experimental half-life of the R-loop divided by the number of steps needed for 50% displacement in a random walk simulation defines the step time required for each individual displacement event along the path. However, this calculation requires a clearly defined start point to yield the correct result. The simulation of the displacement of the above 311 nt RNA reveals a lag phase of ~8000 steps. Experimentally the length of this lag phase fluctuates, since it coincides with the dilution of formamide and the temperature shift from 4 to 37°C. Therefore, we chose to synchronize the experimental data and the simulation results to the time point, or step number respectively, where displacement was first observed. In Figure 4A the synchronized simulation of the displacement of a 311 nt RNA is superimposed with the experimental data derived from the experiment shown in Figures 2A and 3A.

Further analysis confirms that an RNA exchange probability close to 50% is appropriate for this test system. Although heteroduplexes are reported to have reduced thermodynamic stability compared with DNA duplexes, this destabilization is strongly sequence dependent. For sequences of comparable sequence composition, the average step time should be independent of the length of the RNA. The number of steps for a given length RNA is only a function of the RNA exchange probability during the random walk simulation. The appropriate percent probability can therefore be identified as the percentage at which RNAs of different length but comparable sequence composition yield similar step times. Figure 4B shows a plot of calculated step times versus RNA exchange probability for three RNAs ranging from 39 to 545 nt in length. An intercept is found at 50.06% (±0.005%) RNA exchange probability, which translates into a modest destabilization of the heteroduplex relative to its pure DNA counterpart under the applied assay conditions. Table 1 gives a summary of data obtained through restriction digest interference assays and gel shift assays. The average step time calculated for 50.06% RNA exchange probability and three RNAs with comparable sequence composition is 345.0 (±1.3) ms/step.

'Directionality' of exchange: restriction digest interference assay

The random walk simulation and the corresponding calculation of step times is based on the premise that the observed half-live of R-loops is a reflection of the random movement of the migrating branch originating at the beginning of the R-loop, as opposed to multiple scattered dissociation events along the heteroduplex. To confirm this model we measured displacement by a second method which does not rely on complete displacement of the RNA. In this assay, advancement of the migrating DNA branch is measured by the restoration of a restriction site located within the R-loop. This assay was carried out in two variations. First, the restoration of a *Hin*cII site located 39 bp into a small 66 nt R-loop was monitored. The experimental design was based on synthetic oligonucleotides and *in vitro* transcribed RNA as illustrated in Figure 5A. The step time obtained from this experiment was then compared with that obtained with *Eco*RI in the plasmid-based R-loop described in Figure 1. In this second system, the restriction site is located 66 nt from the initial branch point but is part of a 311 bp R-loop. In both cases, 1 min restriction digests using excess enzyme were used to monitor restoration of the restriction site.

Figure 5B shows the result of the *Hin*cII restriction digestion after various times of preincubation. The ratio of product to starting material of this partial digest was scored as a function of preincubation time (Fig. 5C). The scission observed without preincubation time is a reflection of the displacement that occurred during the 1 min restriction digestion. The half-life obtained from this experiment is 5.5 min and the resulting step time is 336.4 ms/step (see Table 1). The half-life obtained with *Eco*RI was 14.9 min and the resulting step time is 326.5 ms/step when calculated for a 66 nt exchange. Hence, for comparable length RNAs and comparable assay conditions the resulting step times are in good agreement. The observed half-lives are a reflection of the distance from the initial branch point to the restriction site and are independent of the total length of the RNA used for R-loop formation. This finding is in good agreement with the proposed model of a 'directional' exchange through a random movement of the migrating branch which has the end of the full-length heteroduplex as its point of origin.

Table 1. Comparison of half-lives and step times (ms/step) for the exchange of different length RNAs in 5 mM magnesium containing buffer

RNA length (nt)	No. of steps (50% EP)[a]	$t_{½}$ (min)[b]	ST (50%) (ms/nt)	ST (50.06%) (ms/nt)	%GC	%U
39	982	5.5	336.4	346.5	58	20
66	2734	14.9	326.5	345.1	60	18
311	63 509	130	122.8	137.3	48	27
545	172 364	632	220.6	343.3	57	22

Data for 39 and 66 nt RNAs (including the full-length restriction consensus site) were determined by restriction digest interference. The sequence composition of the RNAs is described as %GC and %U.

[a]Step times are given from the first exchange to 50% completeness of exchange.

[b]Half-lives were measured from the first signal decay (where applicable) to 50% decay. Step times (ST) are given for 50% RNA exchange probability and 50.06%.

Effect of distamycin on the displacement reaction

In the case of displacement of DNA by DNA the duplexes flanking the migration fork are both DNA duplexes which should exist predominantly as B-form DNA. In the case of RNA displacement by DNA different helix topologies will be found on either side of the branch point. Since heteroduplexes form a helix that is intermediate between A-form RNA and B-form DNA, minor groove binding drugs such as distamycin or netropsin (20–22) should affect the helix stability on either side of the branch point differently. Enhanced stability of both helices will result in increased step times. However, this effect can be overcompensated by a decreased relative stability of the heteroduplex relative to the DNA duplex. The increased RNA exchange probability will result in a dramatic decrease in the number of steps required for complete displacement. This effect is unique to systems containing different species of nucleic acids on competing strands. Distamycin has a K_d for double-stranded DNA in the range of 10^{-6} M and stabilizes DNA, as is evident from an increased melting temperature (23,24). Double-stranded RNA and heteroduplexes are bound very poorly (25). This minor groove binding drug should therefore shift the equilibrium in a random walk mechanism in favor of RNA displacement. Figure 6 shows the effect of distamycin at different concentrations on the time course of displacement of the 311 nt RNA in the presence of magnesium. A significant increase in the rate of displacement can be observed as the distamycin concentration is increased. At 10 µM distamycin, the displacement reaction proceeds so fast that detection of the remaining RNA is only possible immediately after dilution into distamycin-containing buffer. Ethidium bromide produces a similar effect. However, the destabilizing effect is less pronounced and 10 µM ethidium bromide is equivalent to ~1 µM distamycin. This is presumably a reflection of the reduced preference of ethidium bromide for duplex DNA, as is apparent in standard staining techniques, where ethidium bromide is known to bind to double-stranded DNA as well as RNA but is more efficient for the detection of double-stranded DNA.

DISCUSSION

Heteroduplexes consisting of 1 mol RNA and 1 mol DNA form *in vivo* during reverse transcription, DNA replication and transcription. Heteroduplexes also form as a result of the hybridization of antisense deoxyoligonucleotides to mRNA sequences. Mixed sequence heteroduplexes are reported to have a reduced thermodynamic stability compared with double-stranded B-form DNA or A-form RNA. (3–5). In solution, RNA–DNA hybrids are stable, as is evident in the successful use of antisense oligonucleotides. However, RNA can be displaced effectively from these heteroduplexes by homologous DNA strands if the incoming competing strand finds a stretch of template DNA sequence that is not occupied by RNA. This unchallenged annealing step eliminates the otherwise rate limiting nucleation event consisting of spontaneous RNA dissociation and competitive hybridization of DNA and it's attendant unfavorable second order kinetics.

We utilized R-loop formation as a highly specific and efficient method to introduce a segment of RNA into the context of a DNA duplex. R-Loop formation is driven by the higher thermodynamic stability of RNA–DNA hybrids relative to double-stranded DNA in 70% formamide and the tendency of DNA homoduplexes to melt locally under dehydrating solvent conditions (9). Upon removal or dilution of formamide a branch point is established which gradually moves to displace the RNA from the DNA template. Random walk simulations were used to correlate the experimental half-life of R-loops containing RNAs of different length with the step time, the time required for the reversible exchange of a single nucleotide. Displacement proceeds through a random movement of the migrating branch which originates at the end of the full-length heteroduplex. This is evident from the fact that the restoration of an *Eco*RI site, 66 bp from the beginning of the DNA branch point but located within a 311 bp R-loop, is exchanged at a rate characteristic of a 66 nt RNA.

In the presence of magnesium ions the equilibrium between DNA and RNA exchange is close to 50%. Three RNAs of different length but comparable sequence composition (GC content 57–60%, U content 18–22%) show step times from 220.6 to 336.4 ms/step when modeled with a 50% RNA exchange probability. A plot of calculated step times versus RNA exchange probability reveals an intercept at ~50.06% and an average step time of 345.0 (± 1.3) ms/step. This percentage is indicative of a modest destabilization of the heteroduplex relative to the DNA duplex. A deviation towards a shorter step time and less stable heteroduplex is observed with a reduction in the GC content and increased percentage of uracil-containing base pairs. This finding is consistent with the reported thermodynamic properties of heteroduplex base pairs relative to their DNA counterparts. (3,4). Compared with their pure DNA counterparts, rG:dC and rC:dG pairs are more stable than rA:dT pairs (3). Probably due to the inability of poly(rU:dA) tracts to form an A-form helix, rU:dA pairs are exceptionally unstable, about three times less stable than rA:dT pairs (4). An additional cause for the apparent reduction in the average step time can be the formation of secondary structure by the displaced part of the RNA. This can be a considerable

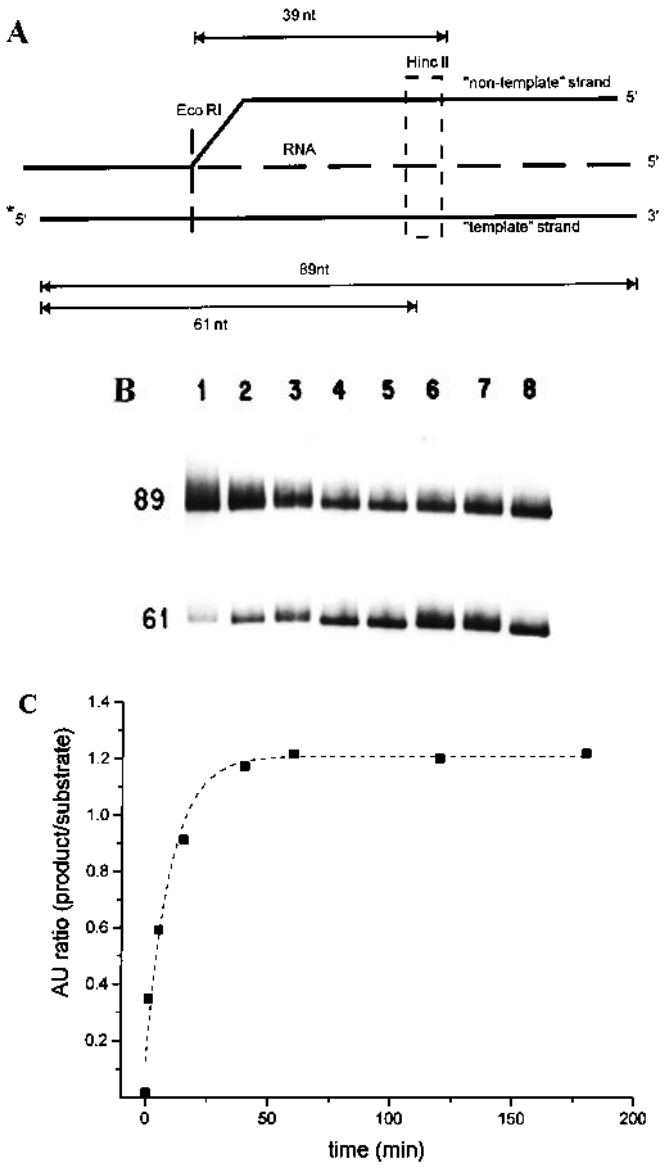

Figure 5. (**A**) *Hinc*II restriction digest interference assay with synthetic R-loop templates. The sequences of the 'template' and 'non-template' strand oligonucleotides are given in Materials and Methods. The oligonucleotides do not contain the T7 promoter information. RNA was generated from *Eco*RI-digested vector pGEM-4 on which the oligonucleotide sequences are based. The location of the 5′-radiolabel on the template strand is indicated by an asterisk. (**B**) Denaturing polyacrylamide electrophoresis of 1 min restriction digests after various times of preincubation at 37°C following formamide dilution. Lanes 1–8, preincubation times at 37°C were 0, 1, 5, 15, 40, 60, 120 and 180 min. The 89 nt substrate and the 61 nt scission product are indicated. (**C**) Ratio of 32 nt product band to 66 nt starting material (determined by densitometry) as a function of total incubation time (1 min restriction digest included).

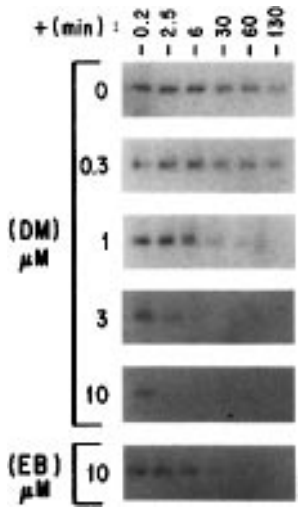

Figure 6. Effect of distamycin on the displacement of a 311 nt RNA in the presence of magnesium as measured by gel mobility shift assay. Decay of the plasmid-associated band is presented for different times of incubation at 37°C. Distamycin (DM) concentrations are shown in μM and time points (top of gel) are given in min. Ethidium bromide (EB) shows a similar effect to DM but is ~10-fold less potent.

source of error for longer RNAs, as it introduces an artificial barrier to the reverse movement in a random walk scheme.

For the 311 nt RNA, the displacement reaction is accelerated ~52-fold in magnesium chloride-free buffer. Exchange for the analogous triple-stranded DNA exchange reaction in the absence of magnesium (15) has been reported to have step times of 12 μs. However, a direct comparison of step times is not possible without knowledge of the correct RNA exchange probability under magnesium-free conditions. The analysis of step times versus RNA exchange probability, as was done in the presence of magnesium (Fig. 4B), is complicated by the rapid displacement of short RNAs. For this analysis new pairs of RNAs, several hundred nucleotides in length, would have to be found which have matching sequence compositions and no strong tendencies towards secondary structure formation. A similar magnesium effect has been reported for strand migration in protein-free models of Holliday junctions. However, for Holliday junctions the increase in the spontaneous strand exchange reaction in the absence of magnesium is much more pronounced (1000-fold) and has been attributed to the stabilizing effect of magnesium on the more complex branch structure of the double junction (26). The increase in exchange rate for the RNA exchange could be explained by destabilization of both types of helices upon removal of Mg^{2+} leading to a higher rate of spontaneous dissociation at the borders of the migrating branch. However, compared with a B-form helix the shallow minor groove of an A-form helix presumably receives no stabilization through magnesium ions (27). The fact that an increase in the exchange rate can be observed might be indicative of a stabilization of the heteroduplex through binding of magnesium in the major groove. A better understanding of the effect of magnesium on heteroduplex stability has to await further structure determination of RNA–DNA hybrids and their magnesium salts.

Because of the cumulative effect of the multiple steps of a random walk mechanism, RNA displacement is extremely sensitive to compounds that preferentially stabilize helices on either side of the migrating branch. As a minor groove binder (20–22), distamycin strongly favors double-stranded DNA over RNA and heteroduplexes which form A-helices. Micromolar concentrations have a substantial stabilizing effect on DNA poly(AT) tracts, but stabilize heteroduplexes only modestly and fail to increase the melting temperature of RNA poly(AU) sequences (25). The addition of micromolar concentrations of distamycin results in a significant increase in the rate of RNA

exchange (Fig. 6). Presumably, distamycin acts as a catalyst for RNA displacement by selective stabilization of the DNA duplex. Although ethidium bromide exhibits a similar effect, distamycin is ~10 times more potent as a 'strand exchange catalyst' because of its stronger preference for double-stranded DNA. This simple assay therefore provides a convenient and sensitive test for the topology-dependent preferential binding behavior of nucleic acid binding drugs and demonstrates a simple model for the 'catalysis' of strand exchange reactions through selective helix stabilization.

The rates of spontaneous displacement of RNA from a heteroduplex are of interest in the context of transcription elongation. At 37°C, RNA polymerase II-catalyzed transcription in *Drosophila* proceeds at ~1100 nt/min (54 ms/nt) (28), poliovirus RNA polymerase catalyzes transcription at ~300 nt/min (200 ms/nt) at 30°C (29) and *Escherichia coli* transcription is reported to be of the order of 30 ms/nt at non-terminator sites *in vitro* (30). As RNA polymerase proceeds along its DNA template, newly synthesized RNA has to be displaced from the short stretch of DNA inside the elongation complex. The length of the heteroduplex in this elongation complex was initially estimated to be ~12 nt long (31,32). Recently this estimate has been challenged by a model of the elongating RNA polymerase–DNA complex that involves as little as 3 bp of heteroduplex (33).

Irrespective of the length of the heteroduplex, displacement of the RNA from the template presents a potentially rate limiting step for fast elongation (i.e. elongation in the absence of specific pause signals) which ranges from 30 to 200 ms/nt. Since the estimated step time for spontaneous exchange in the presence of magnesium is of the order of 300 ms/step, a forward movement at a rate of 300 ms/nt is conceivable merely through stabilization of the DNA helix relative to the heteroduplex. However, in both models proposed above for the mechanism of elongation, the reannealed DNA is unlikely to displace the RNA from the template through direct competition. Alternatively, RNA displacement can be facilitated considerably through omission of magnesium from the short heteroduplex. The rates of displacement observed in the absence of magnesium appear to be fast enough to ensure rates well above those observed for elongation. The exchange reaction could take place in a 'forward only mode' through stabilization of the emerging RNA. Such RNA binding sites can in fact be found on RNA polymerase (34) and binding to these sites is a part of the so-called 'inchworm model' of elongation (33). The rates observed in our assays for the non-protein-catalyzed exchange of RNA from a heteroduplex are therefore in good agreement with a model for elongation that involves only omission of magnesium from the newly synthesized heteroduplex and stabilization of the emerging RNA as the requirements to ensure that RNA displacement is not rate limiting to elongation.

ACKNOWLEDGEMENTS

This research was supported by USPHS grant HG00255 and the award of a Merck Academic Development Program Predoctoral Fellowship CO92591 to R.L.

REFERENCES

1 Lesnik,E.A., Guinosso,C.J., Kawasaki,A.M., Sasmor,H., Zounes,M., Cummins,L.L., Ecker,D.J., Cook,P.D. and Freier,S.M. (1993) *Biochemistry*, **32**, 7832–7838.
2 Jaishree,T.N., van der Marel,G.A., van Boom,J.H. and Wang,A.H. (1993) *Biochemistry*, **32**, 4903–4911.
3 Chamberlin,M.J. (1965) *Fedn Proc.*, **24**, 1446–1457.
4 Martin,F. H. and Tinoco,I. (1980) *Nucleic Acids Res.*, **8**, 2295–2299.
5 Hall,K.B. and McLaughlin,L.W. (1991) *Biochemistry*, **30**, 10606–10613.
6 Kaback,D.B., Angerer,L.M. and Davidson,N. (1979) *Nucleic Acids Res.*, **6**, 2499–2517.
7 Thomas,M., White,R.L. and Davis,R.W. (1976) *Proc. Natl. Acad. Sci. USA*, **73**, 2294–2298.
8 Dickerson,R.E., Drew,H.R., Conner,B.N., Wing,R.M., Fratini,A.V. and Kopka,M.L. (1982) *Science*, **216**, 475–485.
9 Lee,C.H., Mizusawa,H. and Kakefuda,T. (1981) *Proc. Natl. Acad. Sci. USA*, **78**, 2838–2842.
10 Rosbash,M., Blank,D., Fahrner,K., Hereford,L., Ricciardi,R., Roberts,B., Ruby,S. and Woolford,J. (1979) *Methods Enzymol.*, **68**, 454–469.
11 Woolford,J.L.,Jr and Rosbash,M. (1979) *Nucleic Acids Res.*, **6**, 2483–2497.
12 Sigman,D.S., Chen,C.-h.B. and Gorin,M.B. (1993) *Nature*, **363**, 474–475.
13 Landgraf,R., Chen,C. B. and Sigman,D.S. (1995) *Nucleic Acids Res.*, **23**, 3524–3530.
14 Landgraf,R., Chen,C.B. and Sigman,D.S. (1995) *Nucleic Acids Res.*, **23**, 3516–3523.
15 Radding,C.M., Beattie,K.L., Holloman,W.K. and Wiegand,R.C. (1977) *J. Mol. Biol.*, **116**, 825–839.
16 Panyutin,I.G. and Hsieh,P. (1994) *Proc. Natl. Acad. Sci. USA*, **91**, 2021–2025.
17 Dressler,D. and Potter,H. (1982) *Annu. Rev. Biochem.*, **51**, 727–761.
18 Chen,C.-h.B., Gorin,M.B. and Sigman,D.S. (1993) *Proc. Natl. Acad. Sci. USA*, **90**, 4206–4210.
19 Panyutin,I.G. and Hsieh,P. (1993) *J. Mol. Biol.*, **230**, 413–424.
20 Patel,D.J. (1979) *Eur. J. Biochem.*, **99**, 369–378.
21 Coll,M., Aymami,J., van der Marel,G.A., van Boom,J.H., Rich,A. and Wang,A.H. (1989) *Biochemistry*, **28**, 310–320.
22 Klevit,R.E., Wemmer,D.E. and Reid,B.R. (1986) *Biochemistry*, **25**, 3296–3303.
23 Zimmer,C., Reinert,K.E., Luck,G., Wahnert,U., Lober,G. and Thrum,H. (1971) *J. Mol. Biol.*, **58**, 329–348.
24 Zimmer,C. and Luck,G. (1972) *Biochim. Biophys. Acta*, **287**, 376–385.
25 Fillipowsky,M.E., Kopka,M.L., Brazil-Zison,M., Lown,J.W. and Dickerson,R.E. (1996) *Biochemistry*, submitted.
26 Panyutin,I.G., Biswas,I. and Hsieh,P. (1995) *EMBO J.*, **14**, 1819–1826.
27 Skuratovskii,I. and Bartenev,V.N. (1978) *Mol. Biol.* (*Mosk.*), **12**, 1359–1376.
28 LeMaire,M.F. and Thummel,C.S. (1990) *Mol. Cell. Biol.*, **10**, 6059–6063.
29 Neufeld,K.L., Richards,O.C. and Ehrenfeld,E. (1991) *J. Biol. Chem.*, **266**, 24212–24219.
30 Rhodes,G. and Chamberlin,M.J. (1974) *J. Biol. Chem.*, **249**, 6675–6683.
31 Gamper,H.B. and Hearst,J.E. (1982) *Cell*, **29**, 81–90.
32 von Hippel,P.H., Bear,D.G., Morgan,W.D. and McSwiggen,J.A. (1984) *Annu. Rev. Biochem.*, **53**, 389–446.
33 Chamberlin,M.J. (1992) *Harvey Lect.*, **88**, 1–21.
34 Stevens,A. (1969) *J. Biol. Chem.*, **244**, 425–429.